

JUN 10 1984

DATE ISSUED

ORNL/TM-9112

**ornl**

**OAK RIDGE  
NATIONAL  
LABORATORY**

**MARTIN MARIETTA**

MARTIN COPY

**Invention of a Tunable Damper  
for Use with an Acoustic  
Waveguide in Hostile Environments**

Samuel C. Rogers<sup>a</sup>

OPERATED BY  
MARTIN MARIETTA ENERGY SYSTEMS, INC.  
FOR THE UNITED STATES  
DEPARTMENT OF ENERGY

Printed in the United States of America. Available from  
National Technical Information Service  
U.S. Department of Commerce  
5285 Port Royal Road, Springfield, Virginia 22161  
NTIS price codes—Printed Copy: A03 Microfiche A01

This report was prepared as an account of work sponsored by an agency of the United States Government. Neither the United States Government nor any agency thereof, nor any of their employees, makes any warranty, express or implied, or assumes any legal liability or responsibility for the accuracy, completeness, or usefulness of any information, apparatus, product, or process disclosed, or represents that its use would not infringe privately owned rights. Reference herein to any specific commercial product, process, or service by trade name, trademark, manufacturer, or otherwise, does not necessarily constitute or imply its endorsement, recommendation, or favoring by the United States Government or any agency thereof. The views and opinions of authors expressed herein do not necessarily state or reflect those of the United States Government or any agency thereof.

ORNL/TM-9112  
Distribution Category  
UC-37 - Instruments

INSTRUMENTATION AND CONTROLS DIVISION

INVENTION OF A TUNABLE DAMPER FOR USE WITH AN ACOUSTIC WAVEGUIDE  
IN HOSTILE ENVIRONMENTS

Samuel C. Rogers

Date Published: June 1984

Prepared by the  
OAK RIDGE NATIONAL LABORATORY  
Oak Ridge, Tennessee 37831  
operated by  
MARTIN MARIETTA ENERGY SYSTEMS, INC.  
for the  
U.S. DEPARTMENT OF ENERGY  
under Contract No. DE-AC05-84OR21400



TABLE OF CONTENTS

	<u>Page</u>
LIST OF FIGURES . . . . .	iv
ACKNOWLEDGMENTS . . . . .	v
ABSTRACT . . . . .	vii
1. INTRODUCTION . . . . .	1
2. DESCRIPTION OF MEASUREMENT SYSTEM . . . . .	5
2.1 Background Theory . . . . .	5
2.2 Principle of Operation . . . . .	13
3. DAMPER DESIGN AND ANALYSIS . . . . .	15
3.1 Physical Details . . . . .	15
3.2 Mechanism of Operation . . . . .	16
3.3 Distributed System Analogy . . . . .	19
4. RESULTS . . . . .	25
4.1 Test Configuration and Procedures . . . . .	25
4.2 System Performance . . . . .	28
5. SUMMARY . . . . .	31
LIST OF REFERENCES . . . . .	32

LIST OF FIGURES

<u>Figure</u>	<u>Page</u>
1. Ultrasonic level measurement system installed in reactor vessel . . . . .	2
2. Acoustic waves launched in both directions along waveguide . . . . .	3
3. Generation of extensional waves in magnetostrictive rod by the Joule effect . . . . .	6
4. Generation of torsional waves in magnetostrictive rod by the Wiedemann effect . . . . .	6
5. Amplitude attenuation as a function of transmission length . . . . .	12
6. Components of level probe and measurement system . . . . .	14
7. Damper design details . . . . .	16
8. Photograph of damper installed on waveguide . . . . .	17
9. Distributed-parameter representation of a transmission line . . . . .	20
10. Test configuration block diagram . . . . .	26
11. Modified test configuration with damper between extensional and torsional coils . . . . .	27
12. Torsional signal with no damper applied . . . . .	29
13. Torsional signal with damper tuned for torsional mode . . . . .	29
14. Extensional signal with no damper applied . . . . .	29
15. Extensional signal with damper tuned for extensional mode . . . . .	29
16. Torsional signal with damper tuned for extensional mode . . . . .	30
17. Extensional signal with damper tuned for torsional mode . . . . .	30
18. Torsional signal for modified configuration . . . . .	30
19. Extensional signal for modified configuration . . . . .	30

#### ACKNOWLEDGMENTS

The author gratefully acknowledges the support of those persons and organizations whose efforts made possible the invention of the tunable damper. The U.S. Nuclear Regulatory Commission, Office of Nuclear Regulatory Research, sponsored the research that led to this invention; and the Oak Ridge National Laboratory Instrumentation and Controls Division supplied the support necessary to complete the project. R. L. Anderson, W. B. Dress, and G. N. Miller of the Instrumentation and Controls Division made technical contributions to the development of the acoustic waveguide for which the damper was invented.

The author appreciates the guidance and encouragement of S. M. Babcock and W. R. Hamel of ORNL and J. M. Googe, R. W. Rochelle, and J. C. Hung of The University of Tennessee, Knoxville.



## ABSTRACT

A damper was invented to remove undesirable stress pulses from an acoustic waveguide. Designed to be tunable, the damper was constructed to withstand a corrosive or otherwise hostile environment. It serves to simplify the design and enhance the performance of a water-level measurement system, of which the damper and acoustic waveguide are integral parts.

An experimental damper was constructed and applied to an existing level probe and measurement system. The resulting damper, properly tuned, causes acoustic stress pulses that pass into it along the waveguide to be attenuated.



## 1. INTRODUCTION

This report describes the invention of a tunable damper for use with an acoustic waveguide in hostile environments. The damper is a by-product of research sponsored by the U.S. Nuclear Regulatory Commission (NRC) Division of Reactor Safety Research. NRC has issued requirements for water-level instrumentation for use in pressurized water reactor vessels to provide an unambiguous indication of an approach to and recovery from inadequate core cooling. Motivation for this effort stems from the analysis of the accident at the Three Mile Island Nuclear Power Plant, during which a condition of low water level and inadequate core cooling was not recognized for an extended period of time because no direct indication of water level existed in the reactor vessel.<sup>1</sup> The research was conducted at the Oak Ridge National Laboratory (ORNL), which is operated by Martin Marietta Energy Systems, Inc., for the U.S. Department of Energy.

An ultrasonic sensor and measurement system to determine the level of the fluid in which the sensor is immersed has been developed to satisfy the aforementioned requirements, specifically, the water level in a nuclear reactor vessel.<sup>2</sup> A simplified view of a nuclear reactor with the level measurement system in place is shown in Fig. 1. This instrument, described in Sect. 2, depends on the reliable detection and precise time-interval measurement of traveling acoustic pulses and reflections that are introduced into an acoustic waveguide and that propagate along its length. The acoustic waves generated in the waveguide propagate in both directions from the transducer along the waveguide (see Fig. 2). Those traveling in the back-length portion of the waveguide cannot be distinguished from reflected waves of interest returning from the sensing end of the waveguide without special signal conditioning. In the original level sensor design, these undesirable back-end reflected waves were eliminated by using a back length long enough to allow detection of only those echo pulses from the sensor

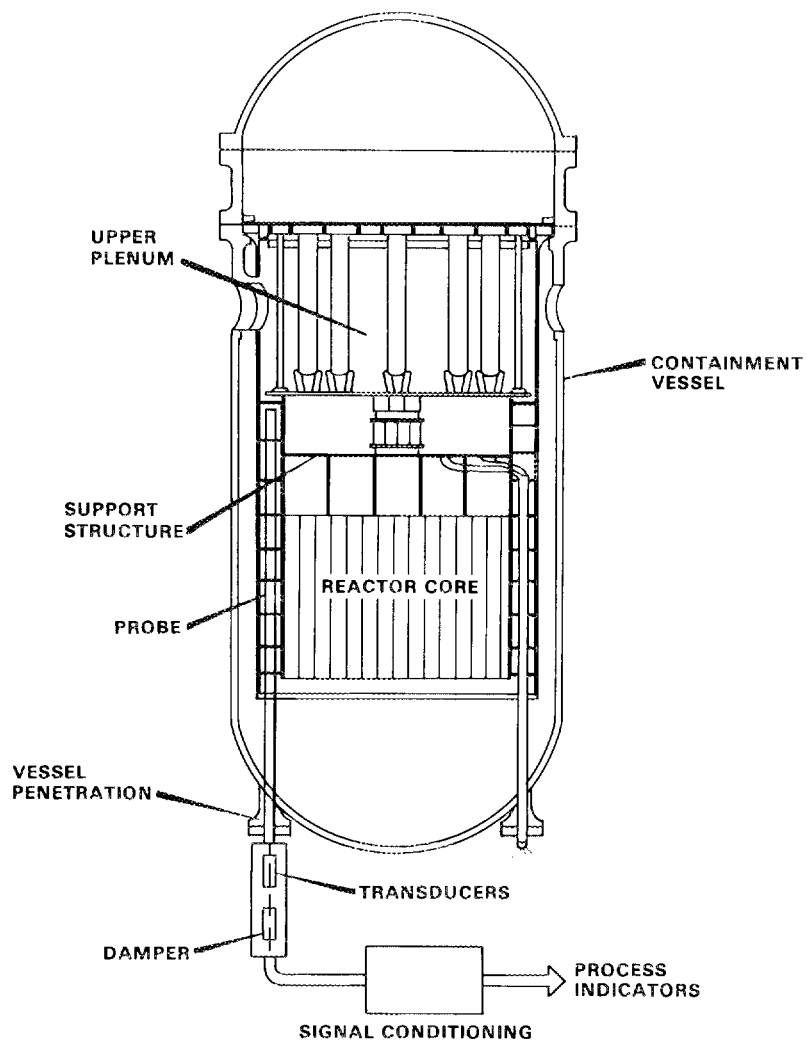


Fig. 1. Ultrasonic level measurement system installed in reactor vessel.

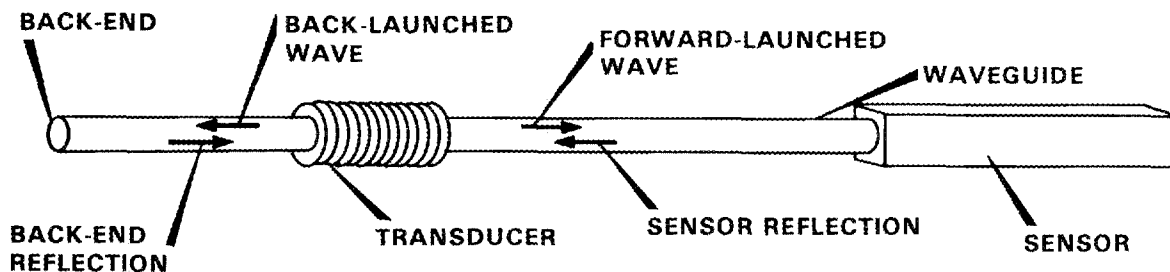


Fig. 2. Acoustic waves launched in both directions along waveguide.

that returned within predetermined time windows. This procedure was unreliable, and it complicated the design of a sensor for reactor applications.

An acoustic damper was therefore designed to remove acoustic wave energy that enters the back-length section of the ultrasonic sensor (acoustic waveguide), thereby simplifying the design and improving the performance of the instrument. Under normal operating conditions, an instrument located inside a reactor vessel would be exposed to temperatures up to 375°C, pressures to 15.2 MPa, flowing water to 20 m/s, and intense nuclear radiation fields. Conventional damper materials such as silicon rubber coating compounds and fiberglass insulation would not withstand such a hostile environment so the damper was constructed entirely of stainless steel; it is thus corrosion and radiation resistant.<sup>3</sup> Furthermore, the damper may be selectively tuned to absorb a given acoustic wave transmission mode and/or frequency, while allowing others to pass.

An experimental damper was constructed and attached to an existing level probe and measurement system. Tests were conducted during which acoustic waves of different modes were passed into the damper along the waveguide, and the damper was tuned until these waves were extinguished. A distributed-parameter system model was subsequently developed to mathematically describe the damper's characteristics.

The following sections are organized to follow generally the development sequence of the acoustic damper. Section 2 sketches the background theory concerning transduction and propagation of acoustic

waves in thin waveguides and describes the general principles of operation of the ultrasonic sensor and measurement system. Section 3, presents a detailed design and intuitive explanation of the damper mechanism, and a mathematical model based on a distributed parameter analogy. Experimental procedures and results are provided in Sect. 4, followed by a summary in Sect. 5.

## 2. DESCRIPTION OF MEASUREMENT SYSTEM

The principles of magnetostrictive generation and propagation of extensional and torsional acoustic stress pulses in thin waveguides are well known and will be briefly described here only as a basis for discussion concerning their application. The operation of the ultrasonic level measurement system is based on the principle that the propagation of torsional acoustic waves in a waveguide of noncircular cross section is retarded by the fluid surrounding the waveguide. Consequently the round-trip transit time of an acoustic wave traveling in the waveguide may be analyzed to yield the density (or level, if the density is known) of the fluid in which the waveguide is immersed. This section deals with the theory underlying the transduction and propagation of acoustic waves in thin waveguides and describes the general operation of the level measurement system.

### 2.1 BACKGROUND THEORY

Extensional and torsional acoustic stress pulses may be generated in magnetostrictive materials by utilizing the Joule and Wiedemann effects, respectively. A current pulse introduced into a coil surrounding a ferromagnetic rod creates a magnetic flux transient in the rod that causes a change in its length by the Joule effect (see Fig. 3).<sup>4</sup> This sudden change in length produces an acoustic stress pulse that at the speed of sound propagates within the material as an extensional wave. Conversely, a returning extensional stress pulse passing under the coil produces a local dimensional change which then generates a change in flux that links the coil. This change in flux produces a voltage across the coil in accordance with Faraday's law.

The Wiedemann effect, or torsional magnetostriction, is a two-dimensional extension of the Joule effect (see Fig. 4).<sup>5</sup> A torsional stress pulse is produced in a magnetostrictive rod when a current pulse is applied to a coil surrounding the rod, causing a magnetic flux

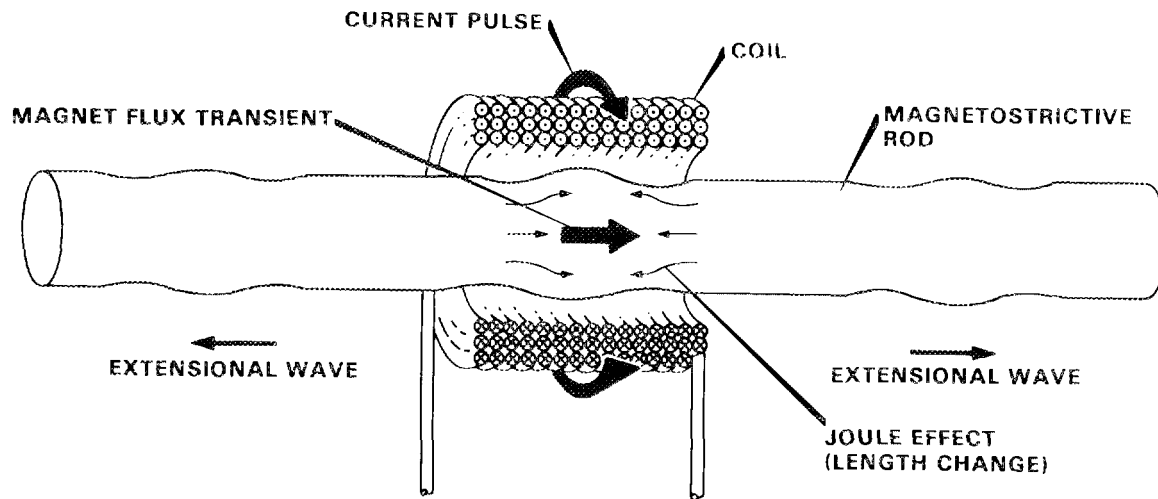


Fig. 3. Generation of extensional waves in magnetostrictive rod by the Joule effect.

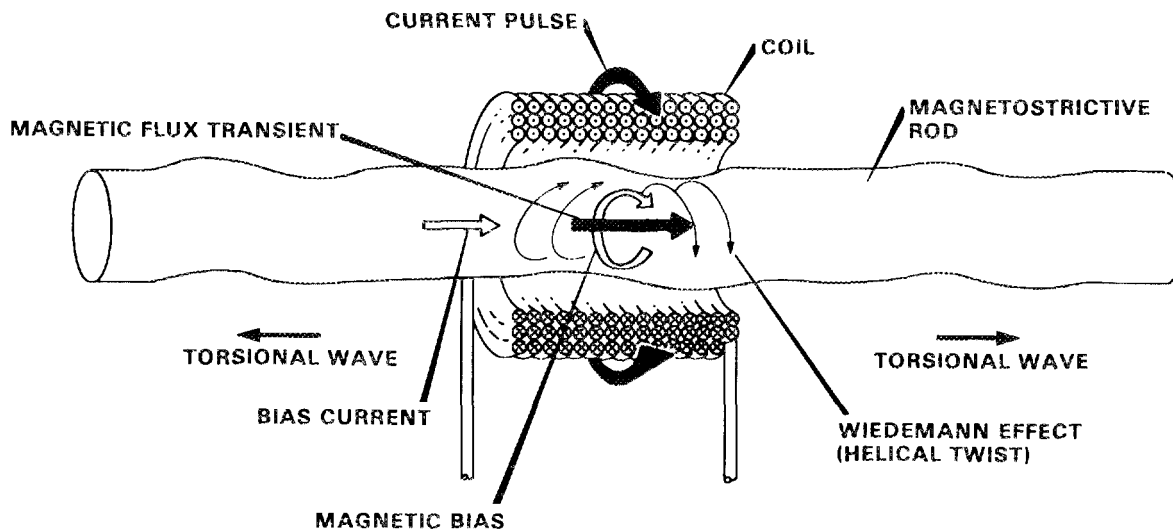


Fig. 4. Generation of torsional waves in magnetostrictive rod by the Wiedemann effect.

transient to interact with an azimuthal magnetic field existing in the rod. Such an azimuthal magnetic bias may be established in the rod by passing a direct current (dc) through the rod. The vector sum of the axially changing flux and the azimuthal bias produces a helical field that twists the rod and initiates a shear stress pulse in the rod. This shear stress pulse propagates as a torsional wave at a speed less than that for the extensional wave. On its return to the coil, the torsional wave produces an output voltage across the coil by the inverse Wiedemann effect and by Faraday's law.

In thin, elastic waveguides, acoustic stress pulses propagate as waves with a phase velocity proportional to the square root of a restoring force, or stiffness term (described by the elastic constants) divided by an inertia term (density or moment of inertia):

$$v = \sqrt{\frac{\text{stiffness term}}{\text{inertia term}}} \quad (1)$$

For a waveguide of noncircular cross section, in a vacuum, the velocity of a dispersionless extensional wave and a dispersionless torsional wave is expressed by

$$v_e = \sqrt{\frac{Y}{\rho_w}} \quad (2)$$

and

$$v_t = K \sqrt{\frac{S}{\rho_w}} \quad (3)$$

respectively. Young's modulus,  $Y$ , and the shear modulus,  $S$ , constitute the stiffness terms. The waveguide density,  $\rho_w$ , represents the inertia term for the extensional mode, whereas  $\rho_w$  and part of the shape factor,  $K$ , together form the inertia term for the torsional mode.

The shape factor,  $K$ , is proportional to the square root of the torsional rigidity constant,  $J$ , divided by the cross-section polar moment of inertia,  $I$ :<sup>6</sup>

$$K = \sqrt{\frac{J}{I}} . \quad (4)$$

For any arbitrary waveguide cross section expressed in rectangular coordinates  $(x,y)$ , the torsional rigidity constant,  $J$ , may be computed by

$$J = \iint F(x,y) \, dx \, dy , \quad (5)$$

where the integrations are taken over the cross section and the function  $F(x,y)$  is equal to zero on the boundary of the cross section and satisfies the nonhomogeneous Laplace equation,

$$\frac{\partial^2 F}{\partial x^2} + \frac{\partial^2 F}{\partial y^2} + 4 = 0 , \quad (6)$$

within the boundary.<sup>7</sup> The cross-section polar moment of inertia may be computed by

$$I = \iint (x^2 + y^2) \, dx \, dy \quad (7)$$

over the same region. For a waveguide of circular cross section,  $K$  is equal to 1; as the geometry departs from a circle,  $K$  becomes less than unity. Utilizing numerical methods and a digital computer,  $K$  was computed for several representative cross-section geometries. The cross-sectional area,  $A$ , polar moment of inertia,  $I$ , torsional rigidity constant,  $J$ , and shape constant,  $K$ , are listed in Table 1 for each geometry. The first three shapes are the unit circle, unit square, and unit equilateral triangle. The subsequent shapes each have arbitrarily chosen 3:1 aspect ratios. The aspect ratio of a waveguide is defined as its greater cross-sectional dimension (width) divided by the equal or lesser orthogonal cross-sectional dimension (height).

Table 1. Constants for shapes representative of waveguide cross-sectional geometrics

Shape	$A^a$	$I^b$	$J^c$	$K^d$
	0.78	1.57	1.57	1.00
	1.00	0.1667	0.1388	0.912
	0.433	0.0361	0.0214	0.770
	1.50	0.625	0.203	0.570
	2.79	2.05	0.649	0.563
	3.00	2.50	0.781	0.559
	1.50	0.646	0.191	0.544
	2.04	0.844	0.235	0.527
	2.17	1.23	0.280	0.477
	1.50	0.813	0.165	0.451

<sup>a</sup>Cross-sectional area.

<sup>b</sup>Polar moment of inertia.

<sup>c</sup>Torsional rigidity.

<sup>d</sup>Shape.

For a waveguide completely immersed in a fluid of density  $\rho$ , the extensional propagation remains essentially unchanged, except for negligible attenuation losses. However, since the torsional motion of a noncircular waveguide is well coupled to the fluid, both energy and momentum are easily transferred to the fluid. The results are not only decreased velocity but also attenuated amplitude caused by the viscosity of the fluid. The fact that the waveguide cross section is noncircular causes inertia from the surrounding fluid to be coupled to the waveguide, thus increasing the effective inertia of the waveguide. Clearly, from Eq. (1), the torsional wave velocity is thereby decreased by a proportional amount. Drag is present but insignificant in rods of circular cross section, so, velocity is virtually unaffected; the viscosity effects however, are substantial. These phenomena are incorporated into an expression by Lynnworth:<sup>8</sup>

$$v_t = K \sqrt{\frac{S}{\rho_w}} \left[ 1 + \frac{\rho}{2\rho_w} \left( 1 - \frac{1}{K} \right) \right]. \quad (8)$$

Equation (8) was empirically determined by analysis of data resulting from experimental studies of the velocity of torsional acoustic waves in rectangular waveguides. However, laboratory tests at ORNL have shown that Eq. (8) is not a valid general expression of the torsional acoustic propagation in arbitrarily shaped waveguides, such as those listed in Table 1. Waveguides with nonrectangular cross sections (triangle, semicircle, and tear shapes) were fabricated and tested. The torsional velocity of propagation was measured for each of the waveguides and found to differ markedly from that predicted by Lynnworth's equation [Eq. (8)]. To the author's knowledge, a correct theoretical expression of the velocity of torsional acoustic propagation in arbitrarily shaped waveguides has not been determined.

Temperature dependence of acoustic stress pulse velocity is a result of the temperature dependence of elastic moduli and density, as well as length, of the waveguide. An increase in temperature decreases both stiffness and inertia terms in Eq. (1). For stainless steel, the

stiffness terms (S and Y) decrease at a rate approximately a factor of 10 greater than the rate for the density term ( $\rho_w$ ). This results in a net decrease in velocity (or increase in transit time) with an increase in temperature for both acoustic wave transmission modes.

The acoustic characteristic impedances of a waveguide are represented by

$$Z_e = \rho_w v_e A = A \sqrt{\rho_w Y} \quad (9)$$

for extensional waves and by

$$Z_t = \rho_w v_t I = \sqrt{IJ\rho_w S} \quad (10)$$

for torsional waves, where A is the cross-sectional area of the waveguide. An impedance mismatch of adjacent sides at a boundary of the waveguide causes an incident wave to be partially reflected (and partially transmitted) at the boundary. The reflection coefficient,  $\Gamma$ , is expressed by

$$\Gamma_{1,2} = \frac{Z_1 - Z_2}{Z_1 + Z_2} \quad (11)$$

Amplitude attenuation of an acoustic wave results from internal absorption losses and from the partial transfer of the wave's energy to an adjacent medium. Laboratory tests have shown that a rectangular waveguide with 2:1 aspect ratio has an attenuation coefficient of 12%/m.<sup>9</sup> Figure 5 is a graph of stress pulse amplitude (electrical representation) versus transmission length. The data are shown fitted to a curve (solid line) with exponential decay. Deviations from this curve are probably due to measurement inaccuracies and to the material and dimensional nonuniformities inherent in such lengthy waveguides. Similar tests of circular waveguides revealed an attenuation coefficient of 10%/m.

A traveling acoustic wave pulse contains a broad, symmetrical spectrum of frequencies about a center frequency,  $f_0$ . The relationship

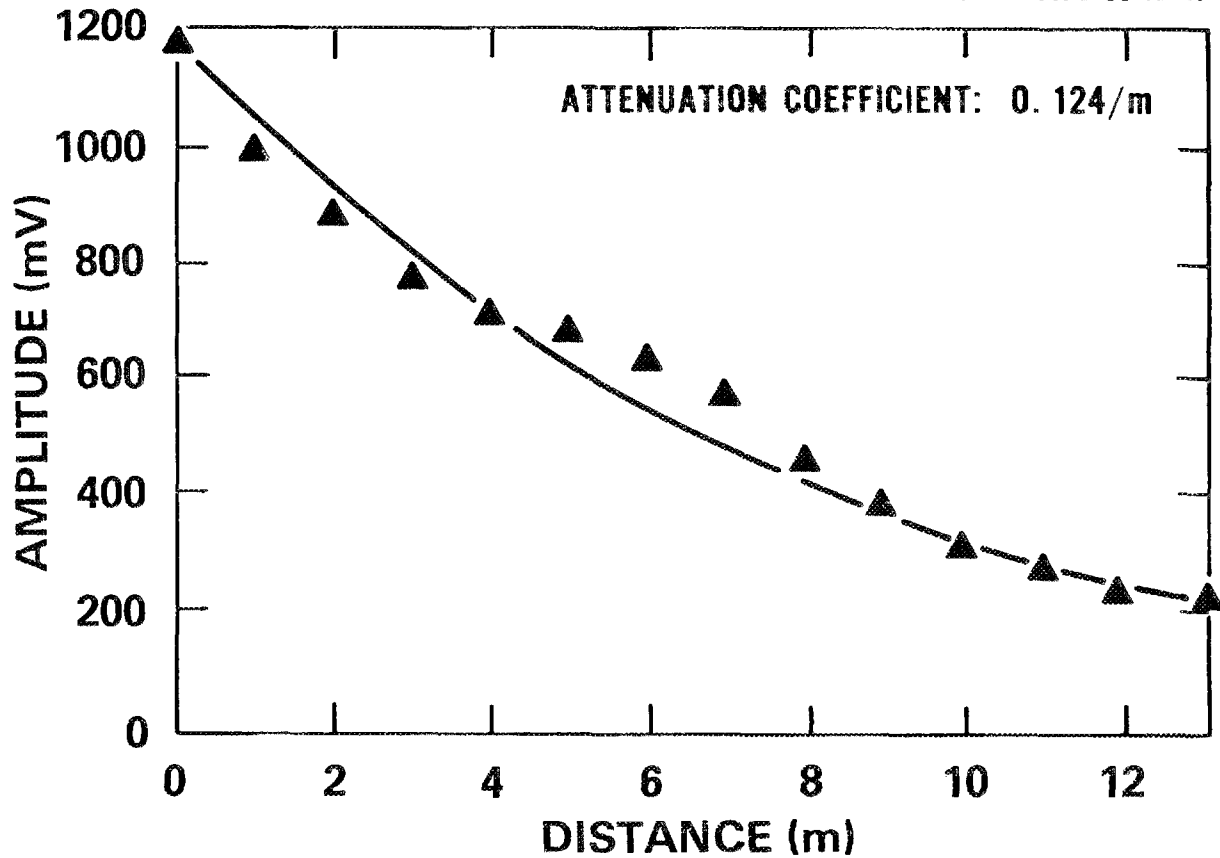


Fig. 5. Amplitude attenuation as a function of transmission length.

that exists among the wavelength,  $\lambda$ , frequency,  $f$ , and velocity,  $v$ , of the traveling wave is expressed by

$$\lambda = \frac{v}{f} \quad (12)$$

Dispersion, or the dependency of velocity on frequency, causes the pulse shape of the wave to spread out in time into many half cycles of pulse amplitude. For dispersionless propagation of the acoustic wave, the ratio of waveguide diameter (or width) to acoustic wavelength must be kept below a critical value,<sup>10</sup> typically 1:8 (hence the expression "thin waveguide"). From experience it is known that maximum energy transfer

and minimum dispersion are obtained when the magnetic coil transducer has a length approximately one-half that of the acoustic stress-pulse wavelength.

## 2.2 PRINCIPLE OF OPERATION

The ultrasonic level probe and measurement system consists of a sensor, a transducer, signal conditioning electronics, and a data processor (see Fig. 6). The sensor is a rectangular stainless steel rod that serves as an acoustic waveguide. Housed in a perforated tube, it is coupled to a transducer by a lead-in waveguide through a sensor/transducer interface. The transducer consists of a 1.6-mm-diam section of magnetostrictive material, such as remendur (composition 49 Co, 2-5 V, bal Fe; permanent magnet alloy with high curie temperature and high residual induction), linked by a pair of magnetic wire coils. The transducer is terminated by a back-length waveguide that is surrounded by the damper. The transducer coils are excited by the signal conditioning electronics, which transmits and receives the signal pulses and provides information to the data processor.

The transducer coils are magnetically biased in such a way that one coil produces extensional acoustic waves while the other produces torsional acoustic waves in the waveguide. The signal conditioning electronics provide current pulses up to 20 A, with widths from 2 to 20  $\mu$ s to each coil in an alternating sequence to launch extensional and torsional acoustic waves in the magnetostrictive rod in each direction from the transducer. Transducer coils of 800 A-turns are sufficient to completely magnetically saturate the remendur. The acoustic waves traveling in the back-length section are absorbed by the damper so as not to be reflected back to the transducer from this end and interfere with the signals from the sensor. Forward-launched acoustic stress pulses propagate in the waveguide through the sensor/transducer interface along the lead-in section to the sensor. Incident waves are partially reflected at the lead-in/sensor interface, at the sensor termination, and at any discontinuities used to divide the sensor into zones at measured intervals along its length. Reflected waves travel back to the

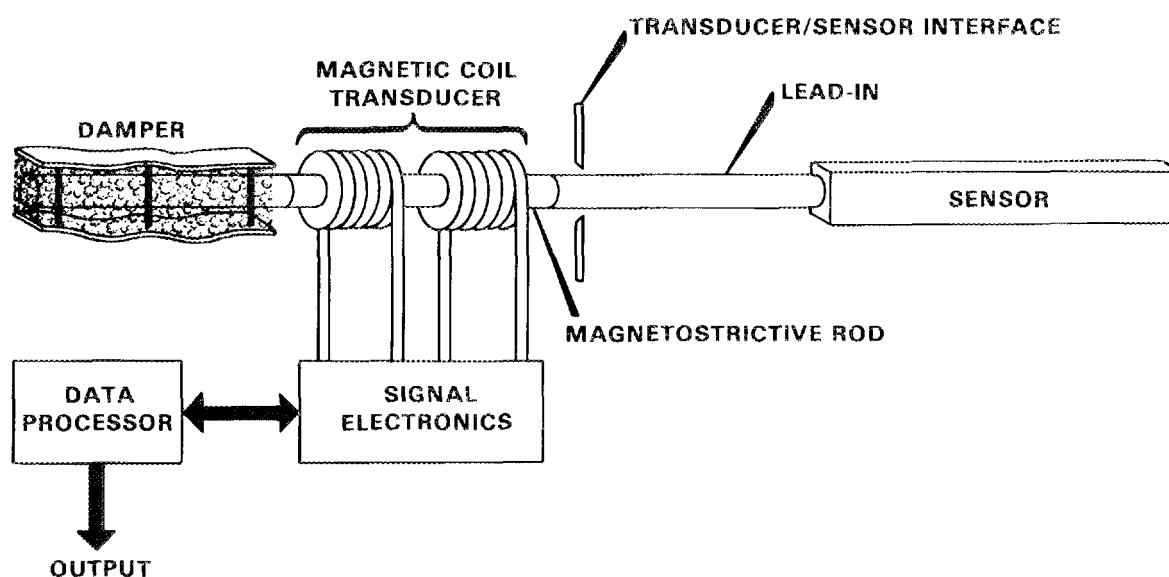


Fig. 6. Components of level probe and measurement system.

transducer coils, where they are converted to electrical signals (up to 2 V peak-peak), received by the signal conditioning electronics, and utilized to measure the round-trip transit time of each wave in the sensor. A nominal value for extensional wave velocity of propagation is 5000 m/s at a waveguide temperature of 25°C. The torsional velocity is less than or equal to this value, depending on the shape factor, temperature, and fluid density effects. For a rectangular waveguide, which has a 2:1 aspect ratio and is immersed in water at a temperature of 25°C, the torsional wave velocity is approximately 3200 m/s.

The measured torsional wave transit time is a function of the density and temperature of the fluid surrounding the sensor. The measured extensional wave transit time is a function of the temperature component of the torsional wave signal only and is used as a temperature compensation factor by the data processor to calculate fluid density, or level.

### 3. DAMPER DESIGN AND ANALYSIS

The requirement that acoustic stress pulse signals from the sensor be readily detectable and unobstructed by spurious back-end wave reflections and prolonged ringing established the need for a means of eliminating interfering back-end acoustic waves from the waveguide. Previous solutions included the utilization of a long back-length section to remove the back-end-traveling acoustic waves in time, and rubber or fiberglass dampers; but these alternatives either compromised the dimensional constraints of the probe or meant the sensor had no chance of surviving nuclear reactor environments. The author's solution to the problem of back-end acoustic waves was an all-metal damper that could withstand the hostile environment of a reactor vessel. An experimental stainless steel damper was therefore designed, fabricated, and tested. This section presents the design details of the damper, describes heuristically the damper mechanism, and concludes with an approximate mathematical model of the damper.

#### 3.1 PHYSICAL DETAILS

Figure 7 is an isometric view of a damper coupled to the back-length portion of an acoustic waveguide. The damper consists of stainless steel wool surrounding a section of the waveguide in which acoustic stress pulse signals are to be damped. The wool that surrounds the waveguide is contained between two rigid stainless steel brackets, which are formed with a sinusoidally bent pattern along their length. The bent pattern has a wavelength approximately equal to that of the acoustic signal to be damped. Although a sine wave pattern is illustrated here, other generally sinusoidal patterns may be employed. The bent pattern of the upper bracket is oriented in phase with the lower bracket pattern. A means, such as clamping screws, is provided to force the plates toward each other and compress the wool against the waveguide. This subjects

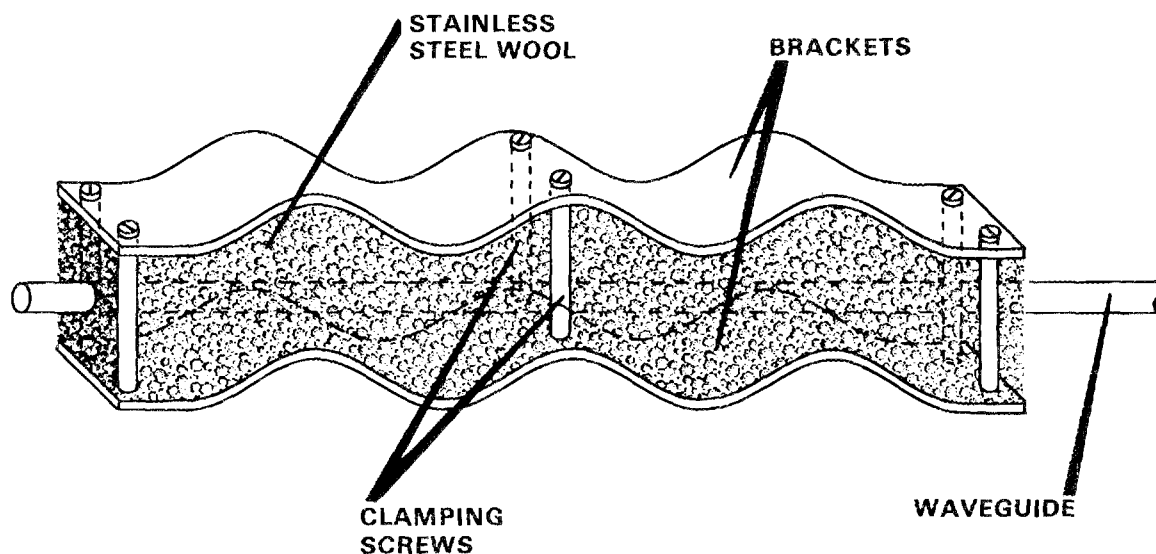


Fig. 7. Damper design details.

the waveguide to alternately opposing lateral bending stresses at  $180^\circ$  intervals along its length in the area to be damped. The bent pattern also produces a pinching effect and provides better coupling of the steel wool to the waveguide.

The experimental damper shown in Fig. 8 was fabricated and applied to a waveguide with a 1.6-mm-diam circular cross section. The damper brackets were 1.6-mm-thick plates, 12.7 mm wide by 203.2 mm in length. The bending pattern wavelength was about 25 mm, compared to the 30.5-mm wavelength of the acoustic waves to be damped. The bent pattern amplitude was about 6 mm peak to peak. The thickness of the steel-wool mass surrounding the waveguide between the sinusoidal brackets prior to compression was about 25 mm. Section 4 summarizes the experimental results of tests conducted on this damper.

### 3.2 MECHANISM OF OPERATION

With no damper present the extensional mode and torsional mode acoustic wave velocity of propagation for an acoustic waveguide in a vacuum may be approximated by

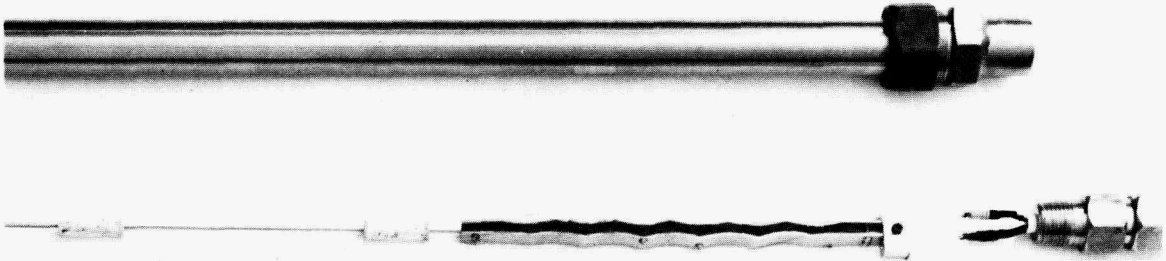


Fig. 8. Damper installed on waveguide.

$$v_e = \sqrt{\frac{Y}{\rho_w}} \quad (13)$$

and

$$v_t = K \sqrt{\frac{S}{\rho_w}} = \sqrt{\frac{JS}{I\rho_w}} \quad (14)$$

These are equations for the velocities of propagation and do not reflect the slight attenuation experienced by such waves in practice. This attenuation is present, even for extensional mode propagation along a waveguide in a vacuum, because of almost negligible internal losses. When the waveguide is immersed in a fluid, such as water, the attenuation becomes more noticeable (10 to 12%/m) because additional energy is dissipated into the fluid as a result of the viscous friction between the

waveguide and the fluid. In the case of torsional mode propagation along a noncircular waveguide immersed in a fluid, drag of the fluid opposes the torsional-wave-induced motion of the waveguide and effectively couples inertia from the fluid to the waveguide. The noncircular geometry aids in the transfer of momentum to the fluid as the apparent inertia of the waveguide,  $I\rho_w$ , is increased, thereby [Eq. (14)] decreasing the velocity of propagation,  $V_t$ .

The damper is applied to a circular section of the waveguide. Because this portion of the waveguide is circular, negligible drag is present and the velocity of propagation is virtually unaffected. Unless the damper is overtuned (excessively tightened), the damper causes no reflection of the incident wave; therefore, the damper does not appreciably alter the characteristic impedance of the waveguide. Also, laboratory tests have demonstrated that the general shape of the acoustic wave is maintained, while the wave's amplitude is diminished by the damper. The velocity of propagation and the characteristic impedance, both of which contain stiffness and inertia terms, are not appreciably affected by the damper because the damper is applied to a circular portion of the waveguide. The mechanism for altering wave velocity and waveguide impedance is drag, which is significantly present only in noncircular waveguides. In circular waveguides, viscous friction is the dominant effect and the mechanism for acoustic wave amplitude attenuation. The damper therefore behaves much like a pure source of viscous friction, acting on the waveguide in such a way that the energy of an acoustic wave propagating in this region is dissipated, resulting in amplitude attenuation only. Viscous friction is supplied to the waveguide as the steel wool is compressed against the waveguide, causing the inhomogeneous, springlike composition of the wool to rub against the waveguide. This effect is more readily obtained for the torsional mode because the damper-waveguide interaction is more direct than that for the extensional mode. In the torsional mode, the waveguide motion is azimuthal, whereas in the extensional mode the motion is both longitudinal and axial (by Poisson's effect) and less easily coupled to the wool.

### 3.3 DISTRIBUTED SYSTEM ANALOGY

The foregoing discussion of the damper mechanism reveals characteristics similar in nature to those of a distributed parameter, linear, distortionless transmission line of infinite length. Though the damper in reality is not an infinite distortionless waveguide, its properties may be approximated to resemble those of a distortionless transmission line, and the damper is therefore modeled as such.

Two essential steps are involved in the analysis of a physical system: (1) the formulation of mathematical equations that describe the system in accordance with physical laws and (2) the solutions of these equations subject to appropriate initial or boundary conditions. In the formulation of equations that describe a physical system, electrical analogies are commonly used because they are easy to symbolize and construct and because special techniques have been developed to analyze them. Nonelectrical systems, such as the damper, have electrical analogies because the equations that describe them are of the same form as those that describe electrical circuits. Transmission lines and acoustic waveguides are examples of distributed-parameter systems. Their component elements are distributed in character, and because more than one independent variable is involved (i.e., time and space), their elements are described by partial differential equations. Elements of lumped-parameter systems, on the other hand, are at most time dependent, and governed by ordinary differential equations.

The classical distributed-parameter electrical circuit model of a transmission line is shown in Fig. 9. Letting

$R$  = resistance per unit length,

$L$  = inductance per unit length,

$C$  = capacitance per unit length, and

$G$  = leakage conductance per unit length,

we have

$$-\frac{\partial e}{\partial x} = Ri + L \frac{\partial i}{\partial t} \quad (15)$$

$$-\frac{\partial i}{\partial x} = Ge + C \frac{\partial e}{\partial t} \quad (16)$$

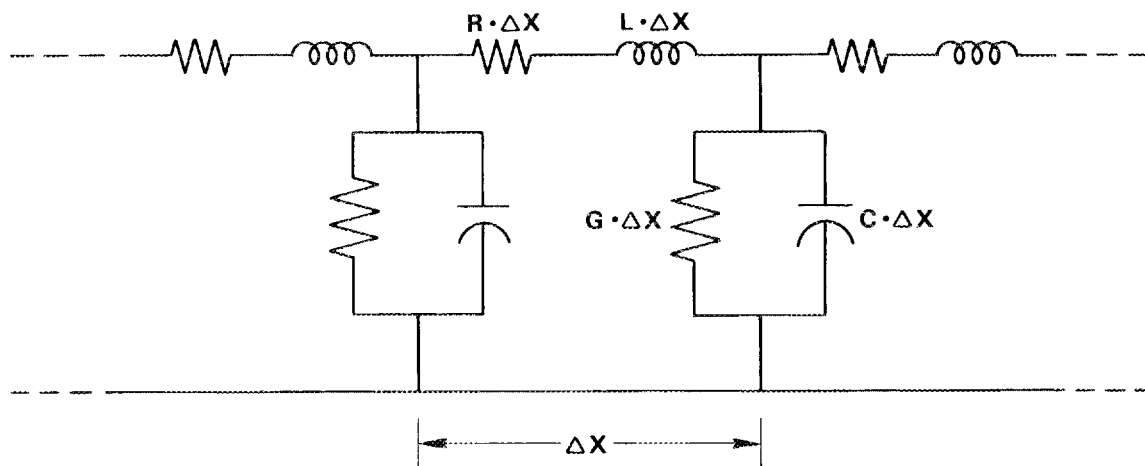


Fig. 9. Distributed-parameter representation of a transmission line. (R = resistance per unit length; L = induction per unit length; C = capacitance per unit length; and G = leakage conductance per unit length.)

Equations (15) and (16) are called "transmission line equations," where  $e = e(x,t)$  is the voltage drop per  $\Delta x$ , and  $i = i(x,t)$  is the current decrease per  $\Delta x$ . The independent variable,  $x$ , is the distance measured from the sending end, and the independent variable,  $t$ , corresponds to time. Differentiating Eq. (15) with respect to  $x$  and Eq. (16) with respect to  $t$ , followed by some rearrangement of the terms, results in the expression

$$\frac{\partial^2 e}{\partial x^2} = LC \frac{\partial^2 e}{\partial t^2} + (RC + LG) \frac{\partial e}{\partial t} + RGe, \quad (17)$$

which is known as a "telegraphist's equation." One method for solving a partial differential equation, such as Eq. (17), is first to convert it into an ordinary differential equation by the Laplace transformation and then to solve the latter by classical methods. Taking the Laplace transformation of Eq. (17), the following is obtained:

$$\frac{d^2 E(x,s)}{dx^2} - \gamma^2 E(x,s) = L \frac{di(x,0)}{dx} - C(Ls + R) e(x,0), \quad (18)$$

where

$$\gamma = \sqrt{(Ls + R)(Cs + G)} \quad (19)$$

is the propagation constant.<sup>11</sup> Assuming zero initial conditions,  $i(x,0) = e(x,0) = 0$ , Eq. (18) reduces to

$$\frac{d^2 E(x,s)}{dx^2} - \gamma^2 E(x,s) = 0, \quad (20)$$

which has the general solution

$$E(x,s) = A e^{-\gamma x} + B e^{\gamma x}. \quad (21)$$

Because  $E(x,s)$  must remain finite even when  $x$  is infinite, it follows from Eq. (21) that  $B = 0$ . If

$$f(t) = e(0,t) \quad (22)$$

is the electrical representation of an acoustic wave introduced into a waveguide where  $x = 0$ , then, from Eq. (21),

$$A = E(0,s) = \mathcal{F}\{e(0,t)\} = \mathcal{F}\{F(t)\} = F(s), \quad (23)$$

thus, the solution to Eq. (20) takes the form:<sup>12</sup>

$$E(x,s) = F(s) e^{-\gamma x}. \quad (24)$$

Approximating the acoustic waveguide without the damper by an analogous lossless transmission line, we have

$$R = G = 0, \quad (25)$$

and, from Eq. (19),

$$\gamma = s \sqrt{LC}. \quad (26)$$

Then, Eq. (24) reduces to

$$E(x,s) = F(s) \epsilon^{-sx} \sqrt{LC} , \quad (27)$$

and the signal propagating in the waveguide may be modeled by

$$e(x,t) = f(t - x \sqrt{LC}) . \quad (28)$$

When the damper is applied to the waveguide, viscous friction is introduced, which is analogous to adding lossy terms,  $R$  and  $G$ , to the transmission line of Fig. 9. Attenuation is the only noticeable effect that the damper has on the wave propagation; there is no change in the velocity of propagation [Eqs. (13) and (14)], in the characteristic impedance [Eqs. (9) and (10)] of the waveguide, or in the shape of the traveling waveform. The inertia and stiffness terms,  $L$  and  $C$ , are not appreciably altered. However,  $R$  and  $G$  must obey a special relationship if the model is to include the characteristic of maintaining the shape of the traveling wave. The acoustic waveguide and damper may thus be approximated by an analogous distortionless transmission line, where

$$\frac{R}{G} = \frac{L}{C} . \quad (29)$$

Then, Eq. (19) becomes

$$\gamma = \sqrt{RG} + s \sqrt{LC} , \quad (30)$$

and Eq. (24) reduces to

$$E(x,s) = F(s) \epsilon^{-x \sqrt{RG}} \epsilon^{-sx \sqrt{LC}} . \quad (31)$$

Therefore, the signal propagating in the region of the waveguide surrounded by the damper may be modeled by

$$e(x,t) = \epsilon^{-x \sqrt{RG}} f(t - x \sqrt{LC}) , \quad (32)$$

where  $x = 0$  is the point along the waveguide at which the traveling wave,  $f(t - x \sqrt{LC})$ , enters the damper. The term  $\sqrt{RG}$  is called the

"attenuation constant;" it is proportional to the amount of viscous friction and internal losses supplied by the damper, causing the otherwise unchanged signal to exponentially decay as it travels over the length of the damper. For values of  $x \sqrt{RG} \geq 4$ , the amplitude of  $e(x,t)$  in Eq. (32) is more than 98% attenuated.

Table 2 is a comparison of analogous equations, expressions, and parameters that exist relative to the electrical transmission line, acoustic extensional-wave propagation in an elastic bar, and torsional wave propagation in a rod of circular cross section.

Table 2. Comparison of analogous systems

Expression	Electrical	Extensional	Torsional
Wave equation (lossless case) <sup>a, b</sup>	$\frac{\partial^2 e}{\partial x^2} = \frac{1}{v^2} \frac{\partial^2 e}{\partial t^2}$	$\frac{\partial^2 E}{\partial x^2} = \frac{1}{v^2} \frac{\partial^2 E}{\partial t^2}$	$\frac{\partial^2 \theta}{\partial x^2} = \frac{1}{v^2} \frac{\partial^2 \theta}{\partial t^2}$
Velocity of propagation, v	$\frac{1}{\sqrt{LC}}$	$\sqrt{\frac{Y}{\rho_w}}$	$\sqrt{\frac{S}{\rho_w}}$
Characteristic Impedance, Z <sub>o</sub>	$\sqrt{\frac{L}{C}}$	A $\sqrt{\rho_w y}$	$\sqrt{IJ\rho_w^s}$
Attenuation constant <sup>c, d</sup>	$\sqrt{RG}$	$\sqrt{\frac{D_e}{f_e}}$	$\sqrt{\frac{D_t}{f_t}}$
Inertia term	L	$\rho_w$	$\rho_w$
Stiffness term	$\frac{1}{C}$	Y	S

<sup>a</sup> E = longitudinal displacement from the equilibrium position of the elastic bar.

<sup>b</sup>  $\theta$  = angular displacement from the equilibrium position of the rod of circular cross section ( $k = \sqrt{\frac{J}{I}} = 1$ ),

<sup>c</sup>  $D_e, f_e$  = lossy terms supplied by damper for extensional mode.

<sup>d</sup>  $D_t, f_t$  = lossy terms supplied by the damper for torsional mode.

## 4. RESULTS

The prototypic damper shown in Fig. 8 was designed, fabricated, and installed on an acoustic waveguide. Tests were conducted in which acoustic waves of different modes were introduced into the waveguide and allowed to pass into the damper. The effects on these signals of tuning the damper were observed and recorded. This section describes the test configuration and procedures and then presents the results.

### 4.1 TEST CONFIGURATION AND PROCEDURES

Figure 10 is a block diagram of the configuration set up for the tests. The waveguide consists of a section of 1- by 2-mm stainless steel ribbon (sensor) welded to a 1.6-mm-diam stainless steel rod (lead-in), whose other end is welded to a 1.6-mm-diam section of remendur. Two magnetic coils surround the remendur to form the transducer, approximately 70 cm from point C (lead-in/sensor interface). A 1.6-mm-diam stainless steel rod (back-length) is attached to the remendur to provide support for the damper. The coils are connected to a Panametrics Panatherm 5010C Ultrasonic Profiler (pulsar/receiver), whose output is monitored on an oscilloscope and recorded by means of a Polaroid camera. A deep-discharge, 12-Vdc, wet-cell battery provides the current necessary to establish the azimuthal bias in the remendur for generating torsional stress pulses; a permanent magnet removes this bias such that extensional stress pulses may be generated in one of the two coils. In a modified test configuration (Fig. 11), the extensional coil is placed at the back end of the waveguide, followed by the damper and the torsional coil. This configuration extends the remendur rod to include the back-length section; the remaining configuration is the same as that shown in Fig. 10.

The Panatherm 5010C pulsar/receiver is programmed first to pulse a selected coil, launching an acoustic wave into the waveguide, and then to receive and amplify the signal produced by the coil as reflected acoustic waves return to the coil. In this way, each coil is excited in an

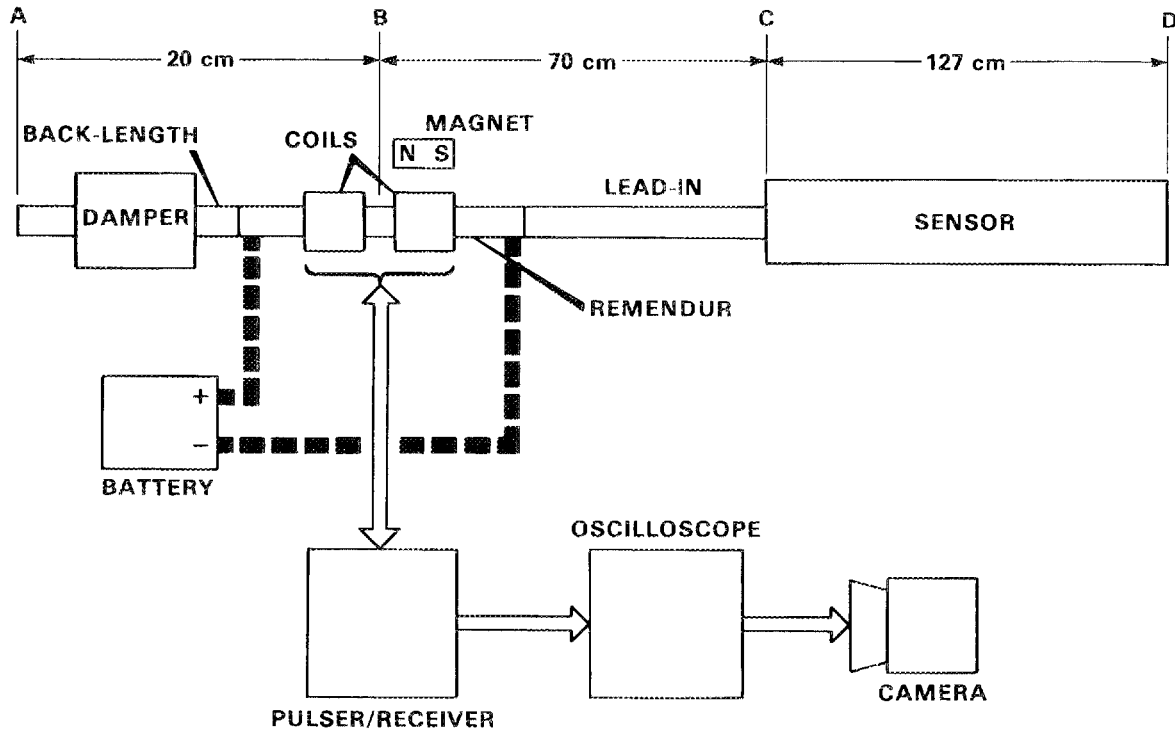


Fig. 10. Test configuration block diagram.

alternating sequence, and the resulting waveforms (electrical representations of reflected acoustic stress pulses) are displayed on the oscilloscope. Additionally, a synchronization pulse is provided by the pulser/receiver, which toggles high/low on alternating pulses to indicate which signal mode, torsional or extensional, is present at the output. This synchronization output is utilized at the oscilloscope's trigger input in such a way that the user may selectively monitor either signal mode by adjusting the negative/positive trigger level switch on the oscilloscope.

The torsional mode was selected for viewing while the damper was tuned. The camera took oscillograms of the torsional mode waveform before the damper was applied and after the damper was tuned to absorb the torsional back-end reflections. Tuning was accomplished by progressively tightening the clamping screws on the damper, while observing the selected waveform, until the back-end reflections' amplitude was reduced to a minimum. (Continued tightening, i.e., overtuning, after the minimum

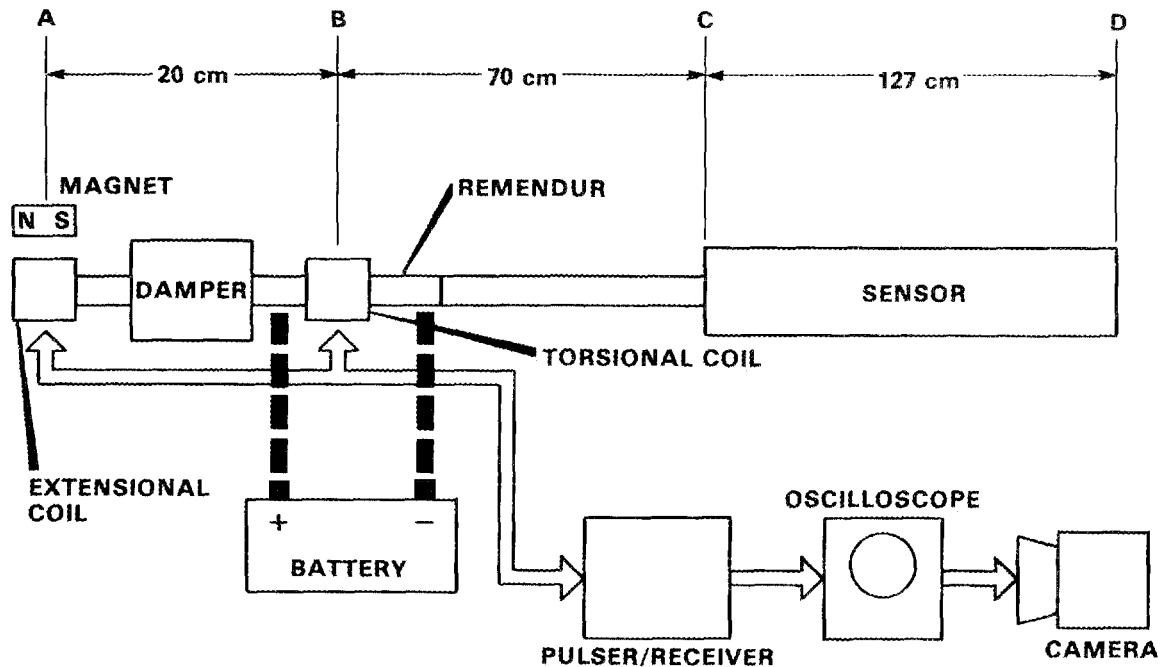


Fig. 11. Modified test configuration with damper between extensional and torsional coils.

is reached can cause the traveling acoustic stress pulses to be reflected by the damper itself.) This procedure was similarly repeated for the extensional mode.

Next, the damper was tuned to eliminate extensional waves, and the torsional mode waveform was recorded. Then, while the damper was tuned to remove the torsional back-end reflections, the extensional mode signals were recorded.

Finally, the modified test configuration in Fig. 11 was implemented, and the damper was tuned to absorb torsional waves. This arrangement allowed extensional-mode stress pulses to pass through the damper and travel on to the sensor, while the damper absorbed torsional mode stress pulses. Extensional back-end reflections were not present, because there was no back-length section behind the extensional coil to sustain them.

## 4.2 SYSTEM PERFORMANCE

The oscillograms from the aforementioned tests reveal the system performance. Figure 12 represents the torsional mode signals present in the waveguide without the damper in use. The voltage spikes are known as echoes and represent traveling acoustic stress pulses that have been reflected at discontinuities along the waveguide and have subsequently propagated back to the originating coil. Echoes  $\alpha$  and  $\beta$  (Fig. 12) are the signals of interest that were reflected at points C and D (Fig. 10), respectively, from the sensor boundaries. The other echoes in Fig. 12 are the undesirable reflections from the back-end of the waveguide. Figure 13 is the same torsional signal except that the damper was tuned to eliminate the back-end echoes. Only the desired signals from the sensor, echoes  $\alpha$  and  $\beta$ , are present. Similar results for the extensional mode are found in Figs. 14 and 15. Figure 14 shows noise corrupted extensional mode echoes with no damper applied, whereas only signal echoes  $\gamma$  and  $\phi$ , from points C and D, respectively, are dominant in Fig. 15 after tuning the damper. Elimination of the extensional mode back-end echoes required more tightening of the damper clamps than that required for the torsional mode. With the damper tuned for the extensional mode, the torsional mode waveform was reexamined. As can be seen in Fig. 16, the torsional back-end reflections remain damped. By contrast, when the damper is tuned to eliminate torsional mode reflections, extensional mode back-end echoes are only slightly damped (see Fig. 17). Thus, it is possible to tune the damper to filter torsional stress pulses while allowing extensional stress pulses to pass. However, additional damping is required to absorb extensional stress pulses, and the torsional mode signals are simultaneously absorbed. The test configuration was therefore modified (see Fig. 11) to take advantage of selective filtering. With the extensional coil on the back-end of the waveguide, no back-end reflections are in a position to interfere; furthermore, forward-launched extensional stress pulses pass through the damper tuned for the torsional mode, whereas torsional mode stress pulses traveling in the back-length are absorbed by the damper. The results of this configuration are shown in Figs. 18 (torsional signals  $\alpha$  and  $\beta$ ) and 19 (extensional signals  $\gamma$  and  $\phi$ ). This method produces very clean signals in both

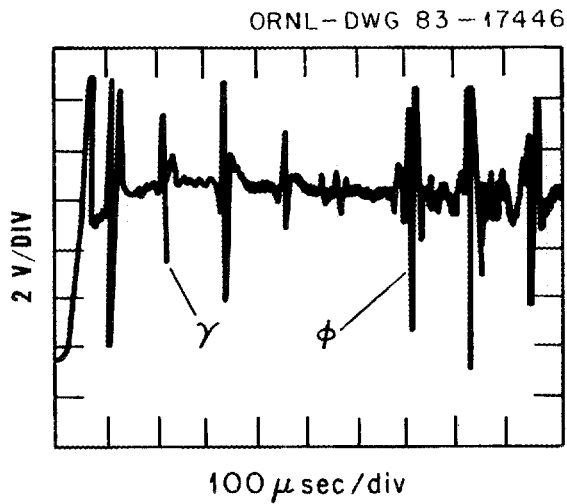


Fig. 12. Torsional signal with no damper applied.

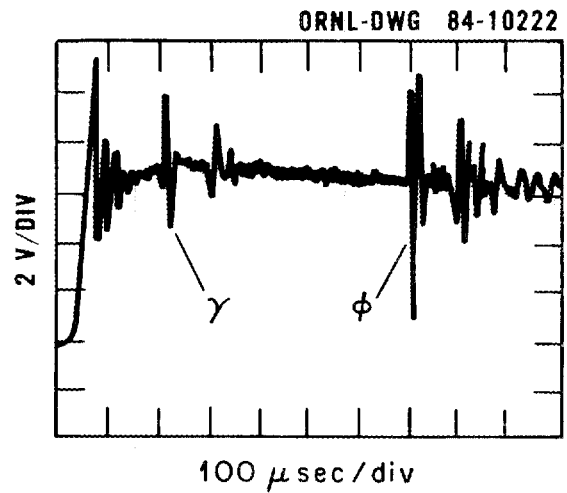


Fig. 13. Torsional signal with damper tuned for torsional mode.

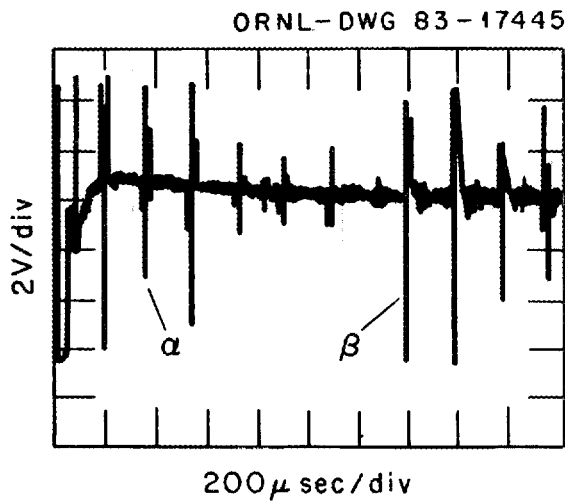


Fig. 14. Extensional signal with no damper applied.

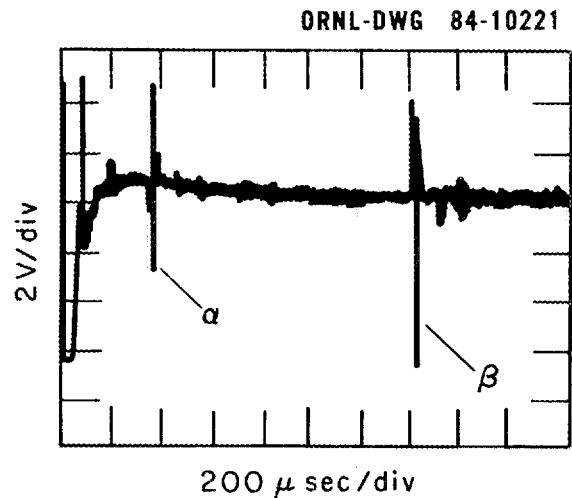


Fig. 15. Extensional signal with damper turned for extensional mode.

modes, optimizing dual-mode performance. It is thus the preferred method of operation, and it has produced good results in practice with a working measurement system.

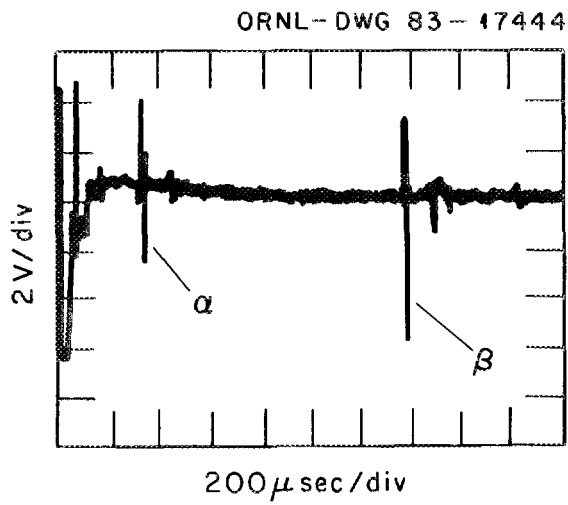


Fig. 16. Torsional signal with damper tuned for extensional mode.

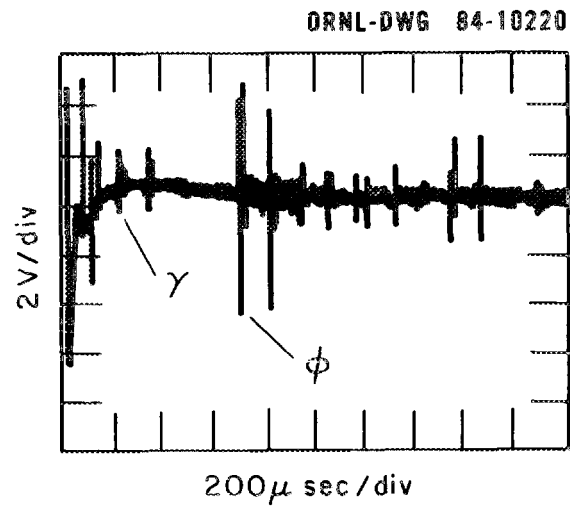


Fig. 17. Extensional signal with damper tuned for torsional mode.

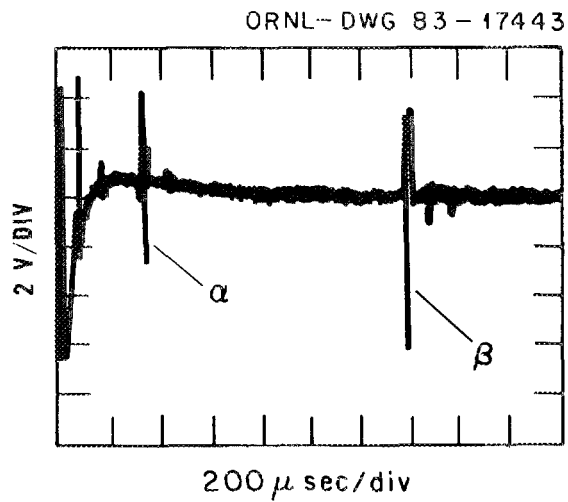


Fig. 18. Torsional signal for modified configuration.

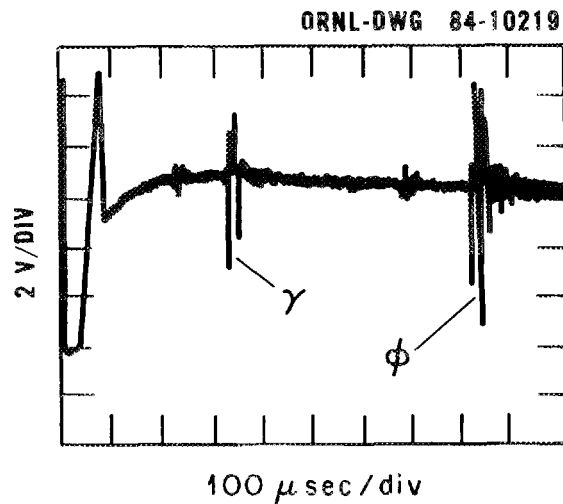


Fig. 19. Extensional signal for modified configuration.

## 5. SUMMARY

A damper that removes undesirable stress pulses from an acoustic waveguide was successfully designed, constructed, and experimentally verified. A mathematical model was then developed to describe the damper's behavior in terms of an analogous distributed-parameter transmission line. The damper serves to simplify the design and improve the performance of an ultrasonic water-level measurement system. It is a by-product of research conducted at ORNL to develop advanced instrumentation for use in pressurized-water reactors.

The damper possesses several salient features that contribute to its uniqueness. Constructed entirely of stainless steel, it is capable of surviving in the hostile environment of a nuclear reactor, whereas previous state-of-the-art designs utilized materials that failed under such conditions. The damper is tunable, which increases its flexibility for use in other more general applications. A simple design makes it easy to construct, and its self-contained, compact structure allows the damper to be applied as an integral part of the acoustic waveguide.

Acoustic stress pulses that propagate along the back-length section of the waveguide and enter the damper are sufficiently attenuated. In this way, back-end reflections of the acoustic waves are prevented from interfering with signals received from the sensor portion of the waveguide, simplifying the pulse-echo discriminating electronics. Reverberations of acoustic waves with the back-end are likewise eliminated, reducing the ringing effect and increasing the upper limit of the transducer excitation repetition rate, which increases the rate at which signal information is gathered, extends the instrument's bandwidth, improves correlation between torsional and extension modes, and sharpens resolution. Utilizing a damper rather than simply extending the back-length section reduces the probe length by greater than a factor of 2, which facilitates installation by keeping the probe within dimensional constraints of present reactor designs.

## REFERENCES

1. *TMI-2 Lessons Learned: Task Force Status Report and Short Term Recommendation*, NRC Report NUREG-0578, pp. A-11 and 12 (July 1979).
2. S. C. Rogers and G. N. Miller, *IEEE Trans. Nucl. Sci.*, NS-29 (1), 665-668 (February 1982).
3. G. N. Miller, et al., *Ultrason. Symp. Proceedings*, IEEE, 2, Cat. 80CH1602-2, pp. 877-881 (October 1980).
4. N. S. Tsannes, *IEEE Trans. Sonics Ultrason.*, SU-13, (2), 33-41 (July 1966).
5. R. M. Bozorth, *Ferromagnetism*, D. Van Nostrand Co., New York, 1951.
6. S. Spinner and R. C. Valore, *J. Nat. Bur. Stand.*, 60, (5), Research Paper 2861 (May 1958).
7. G. Pickett, "Equations for Computing Elastic Constants from Flexural and Torsional Resonant Frequencies of Vibration of Prisms and Cylinders," *Proceedings Am. Soc. Test. Mater.*, 45, 846 (1945).
8. L. C. Lynnworth, *Ultrason. Symp. Proceedings*, IEEE, Cat. No. 77CH1264-ISU, pp. 29-34 (1977).
9. W. B. Dress, *A Torsional Ultrasonic Technique for LWR Liquid Level Measurement*, NRC Report NUREG/CR-3113, ORNL/TM-8585, pp. 2 and 3, (January 1983).
10. S. Davidson, "Wire and Strip Delay Lines," *Ultrasonics* (July-September 1966).
11. D. K. Cheng, *Analysis of Linear Systems*, Addison-Wesley Publishing Co., Reading, Mass. 1959.
12. Stanford Goldman, *Transformation Calculus and Electrical Transients*, Prentice-Hall, Englewood Cliffs, N.J., 1949.

ORNL/TM-9112  
Distribution Category  
UC-37 - Instruments

Internal Distribution

- |        |                      |        |                                    |
|--------|----------------------|--------|------------------------------------|
| 1.     | R. L. Anderson       | 21.    | P. F. McCrea (Advisor)             |
| 2.     | S. M. Babcock        | 22.    | P. W. Murrill (Advisor)            |
| 3.     | B. G. Eads           | 23.    | H. M. Paynter (Advisor)            |
| 4.     | J. M. Googe          | 24.    | H. E. Trammell (Advisor)           |
| 5.     | W. R. Hamel          | 25.    | ORNL Patent Office                 |
| 6.     | G. N. Miller         | 26-27. | Central Research Library           |
| 7.     | C. A. Mossman        | 28.    | Y-12 Document Reference<br>Section |
| 8.     | F. R. Mynatt         | 20-30. | Laboratory Records Dept.           |
| 9.     | R. W. Rochelle       | 31.    | Laboratory Records ORNL-RC         |
| 10-19. | S. C. Rogers         | 32.    | I&C Publications Office            |
| 20.    | M. J. Kopp (Advisor) |        |                                    |

External Distribution

33. Assistant Manager for Energy Research and Development, DOE-ORO, Oak Ridge, TN 37830.
- 34-196. Given distribution as shown in TID-4500, Category UC-37, Instruments.